

FAINTSTAR: A smart single-chip image sensor for next generation star trackers

Werner Ogiers⁽¹⁾, Steeve Kowaltschek⁽²⁾, Jeroen Hoet⁽¹⁾, Jan Vermeiren⁽¹⁾

⁽¹⁾*Caeleste cvba, Hendrik Consciencestraat 1 b – 2800 Mechelen – Belgium, +32 15 71 05 03, werner.ogiers@caeleste.be*

⁽²⁾*ESA-ESTEC, Keplerlaan 1 – 2201 AZ Noordwijk – The Netherlands, +31 71 565 6565, steeve.kowaltschek@esa.int*

Abstract

Since early 2000, the development of smart star tracker image sensors is included on the ESA detector roadmap. FAINTSTAR is the latest development in a successful chain of devices; it has 1024*1024, 4T pixels on a pitch on 10 μm and it is operated in rolling shutter mode with CDS. The full well charge of the pixel is 110 ke⁻ with a noise floor of 21 e⁻_{rms}. The analog signal of each pixel is converted with column AD converters. All bias voltages and currents are generated on-chip. When reading out the raw image data in 12-bit mode a frame rate of almost 12 fps can be achieved. The data are transferred, and the sensor is controlled via a SpaceWire interface.

Much higher frame rates can be achieved when the image sensor is used in windowed mode, where a box around the selected stars is read out. The windowing capabilities are very flexible: 2 sets of windows can be defined; each set can have a different window size and integration time, allowing the simultaneous tracking of bright and faint stars.

More important is the signal processing capability of the image sensor. The Hard-wired processing unit with parametrized functions in conjunction with a 160 kbit SRAM can perform most operations related to star centroiding.

Notwithstanding all the above features, the power dissipation is limited to [250 - 320 mW]. The chip is designed completely in a RadHard by Design (RHbD) way. The space qualification was executed according to the ESC-9020 standard.

1. INTRODUCTION

FaintStar (FS) is a system-on-chip CMOS image sensor with digital signal processing and memory. Its application field encompasses attitude and orbit control systems (AOCS), i.e., star trackers and navigation cameras. As part of the ESA AOCS roadmap, FaintStar was conceived to be the next-generation star sensor, succeeding the older STAR1000, LCMS and HAS2 devices [1-2].

From 2008 on ESA has been planning the next generation of navigation sensors, following two different roads: one road aimed purely at electro-optical performance, the other road aimed at adding more functionality to the chip, in support of a future class of miniature optical heads for star trackers. On this second road lies the FaintStar: a system-on-chip combining improved electro-optical performance with the bulk of the data processing required for star and sun sensing.

2. ARCHITECTURE

The image sensor part of FaintStar consists of a one-megapixel monochrome pixel matrix on 10 μm pitch; the pixels are operated in rolling shutter mode. As Faintstar is a camera-on-a-chip with a high degree of function integration, all interaction with the host system is over a single 40 or 80 Mb/s SpaceWire channel [3]. There are various readout modes for the pixel array (full frame, windowed,

windowed with dual rolling shutter, ...). Raw image output is also supported: uncompressed, JPEG, or run-length encoded.

Hardwired 'pixels-to-centroids' digital image processing encompasses transfer curve linearization, bad pixel replacement, background estimation and subtraction, spike filtering, star image extraction, and photometric barycenter calculation. The chip contains system-level components, including two 1.8V regulators, power-on-reset, temperature-sense diode, analogue inputs with 10-bit conversion, and digital GPIO.

Figure 1 shows the chip block diagram, with analogue sensor core and ADCs, logic core, ancillary blocks, and input/output (IO).

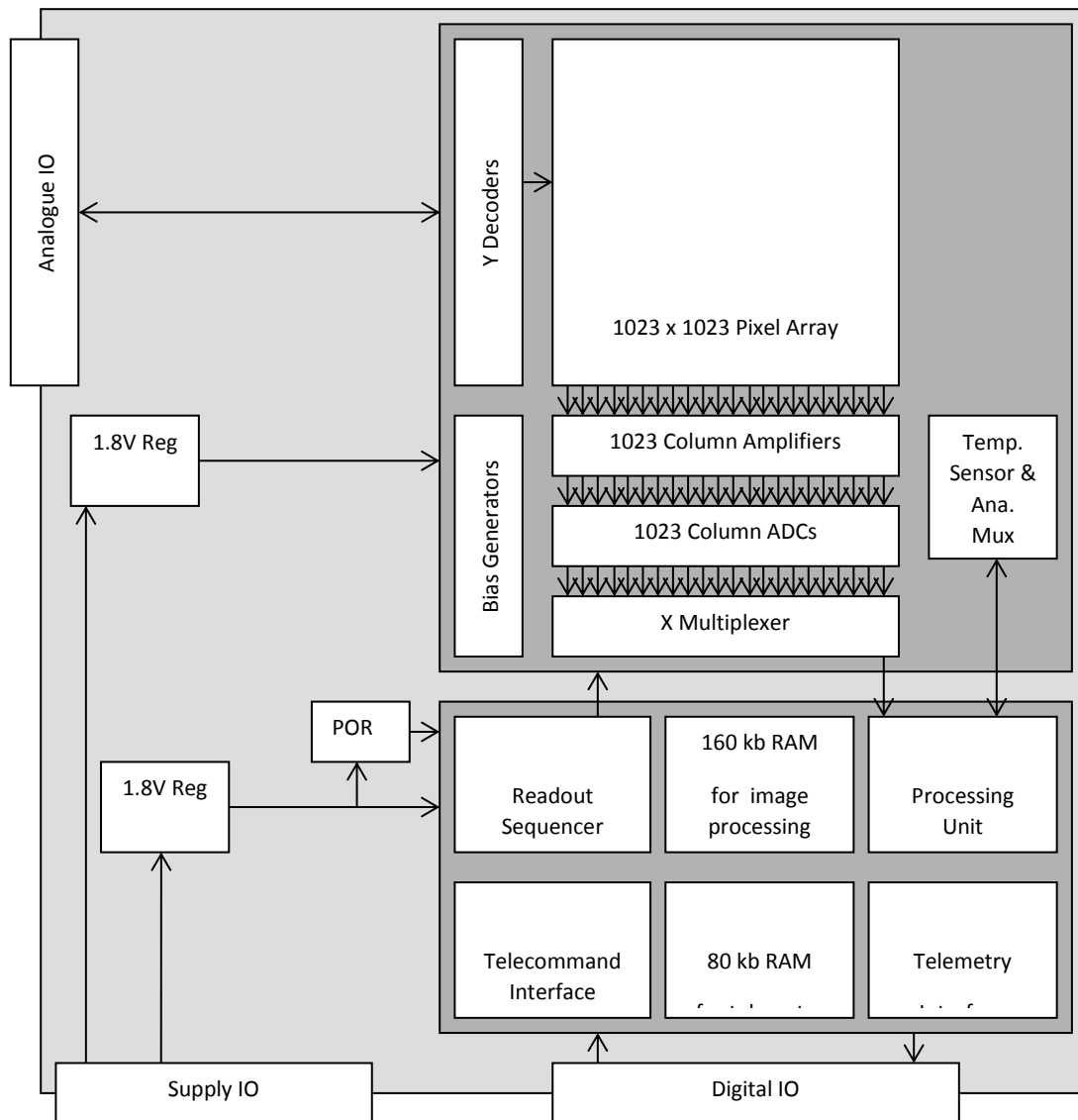


Figure 1: Functional floorplan of the Faintstar SoC image sensor

The image sensor area has 1023x1023 buried photodiode 4T pixels of 10x10 μm . The exposure is executed in Rolling Shutter mode. All necessary bias voltages and currents are generated on the chip.

Each pixel line is sequentially fed into a bank of 1023 ramp ADCs with 12-bit resolution (with an 11-bit option for faster readout). The pixel data are serialized and further processed in the processing logic, where the raw-encoded ADC output is converted to 12-bit positive video.

All communication is through a SpaceWire telecommand/telemetry (TC/TM) interface with LVDS or CMOS signal levels, and a 2x3 bit General Purpose Input Output (GPIO) port. Telemetry can be buffered in an 80 kb First-In First-Out buffer (FIFO).

A local 10-bit ADC digitizes the temperature sensor as well as of six analogue input channels with a rail-to-rail input range (ground to 3.3 V).

The analogue image sensor core and the ADC analog front-ends require a 3.3 V domain. The ADC digital back-ends, the logic, and the RAMs are operating in a 1.8 V domain. There are two 3.3 V-to-1.8 V 100 mA linear regulators on the chip, to be used when the external pin count needs to be minimal. As these regulators add considerably to the on-board power dissipation, off-chip DC/DC convertors may be a better option for high-performance systems.

The power-on-reset circuit (POR) is connected to the core 1.8 V logic supply. The chip is operated from an external 40 MHz or 80 MHz clock source, resulting in external data rates of 40 Mbps and 80 Mbps respectively. The core logic always runs at 40 MHz. The highest internal pixel rate is 13 megapixel/s. The highest external pixel rate, using SpaceWire raw image telemetry, is 5 megapixel/s (12 bit) or 8 megapixel/s (8 bit).

3. SYSTEM-ON-A-CHIP WINDOWED MODE

Besides of the regular imaging mode, the FaintStar sensor can also be used as a full System-on-a-chip (SoC), where the sensor takes over most of the signal processing functions, as depicted in Figure 2.

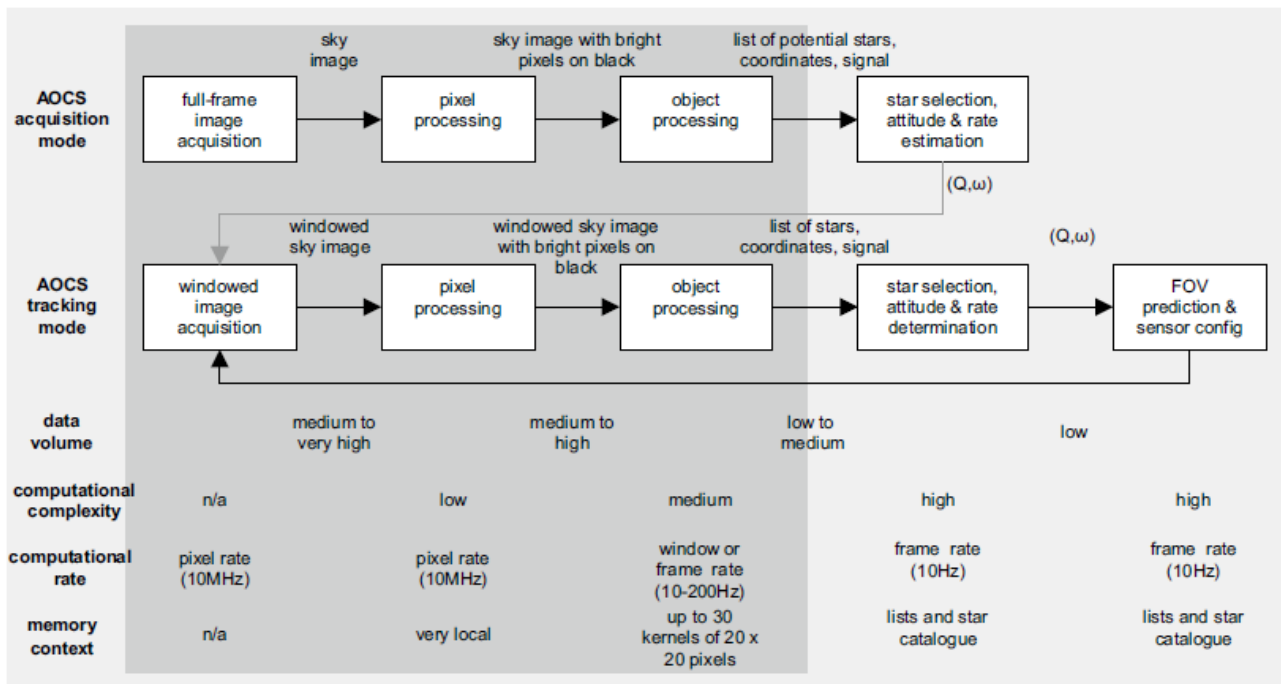


Figure 2: Block diagram of star tracker function, including the repetition rate and the computational complexity. The darker shaded functions can be executed in the Faintstar image sensor.

In windowed or SoC mode up to 30 windows can be defined for start position extraction. Each window can belong to one of the two window classes, named primary and secondary class. All the windows in a class have the same dimensions (between 8×8 and 255×255 pixels) and the same exposure time.

Between the two classes the dimensions and exposure time can differ (thanks to the dual rolling shutter). Windows of differing classes must not overlap each other in the vertical direction (see Figure 3).

Windows can be moved around in the FOV dynamically during readout. This is done without interrupting the image acquisition, and thus, the frame rate will be the highest, but, depending on the window position, some pixel integration times can be corrupted by the window reallocation, when this is coinciding with the line reset time. Windows can also be repositioned statically, by halting the readout, reconfiguring the sensor, and then restarting exposure and readout (so-called one-shot operation). In this case, no data are disturbed, but the attainable frame rate is lower.

Windowed mode is typically used for tracking, with many P(rietary) windows aimed at the guide stars, and one or a few S(econdary) windows aimed at larger celestial bodies in the FOV.

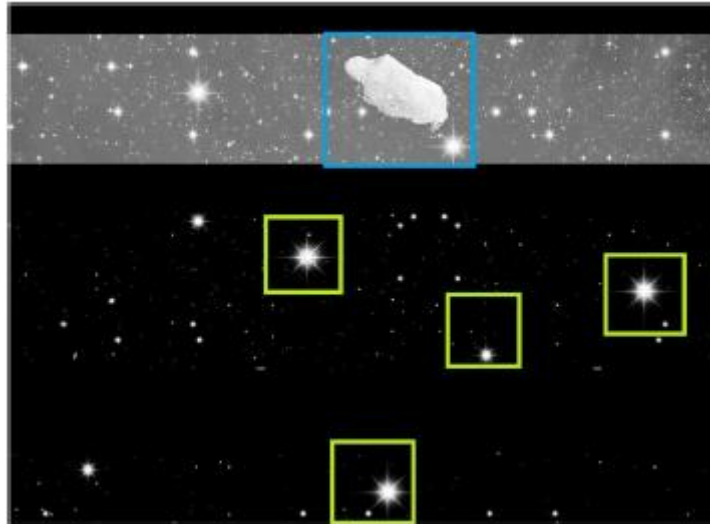


Figure 3: Synthetic image showing regional shutter and windowing: frame with primary (green) and secondary (blue) windows. Only the pixels enclosed by the windows are read. Lines not belonging to any window are skipped.

The prime purpose of the signal processing is to detect starlike bright objects in the images and calculate their photometric centroids (Figure 3). FaintStar data processing is all hard-wired, and there is no software-programmable component on the chip. In order not to limit the design up-front, all functions are highly parameterized (approximately 400 accessible parameters), and in some cases, alternative methods were implemented, giving the end-user some options for customization at the application level [4].

For reasons of design safety, the primary processing functions, i.e., those contributing to the light-to-centroids transform, were made without reliance on the on-chip RAMs. All algorithms considered simultaneously only pixels on the same line. Most processing functions are dedicated to star tracking: background estimation and subtraction are used to remove straylight from the field of view, rendering all bright pixels of interest (stars) against a level backdrop. There are four background estimation methods. All methods have user-programmable bright pixel thresholding at their inputs, keeping star signal from contaminating the background average.

The next step is single illuminated-pixel (SIP) removal. SIPs are solitary pixels that stand out from the background by their brightness, whereas star images are defocused and thus do not give solitary bright pixels. SIPs are caused by high-energy photons and particles, radiation defects or by heat (local dark current hot spots). They are removed by a one-dimensional median filter with programmable thresholds.

The final pixel processing stage is thresholding, where pixel values above a set value pass, and below that level are reset to zero. This results in a black image with only grey values, where presumed star images are.

This cleaned-up image then enters object processing. X-contiguous bright pixels are grouped into one-dimensional bright segments, and Y-contiguous segments are grouped into two-dimensional bright clusters. Once a bright object has been fully isolated from the background, it is immediately evaluated according to user-specified criteria. Clusters fulfilling the criteria pass on to centroiding. Multiple sets of criteria can be predefined and then assigned to individual windows, tailoring each window to the magnitude of the expected star. The centroids are calculated with the moments' method, with an accuracy of 18 bits (1/256th of a pixel).

4. REALIZATION

The analogue blocks were designed as full custom layouts. The analogue parts use TID resistant Enclosed Layout Transistors where appropriate. The counters in the ADCs are Triple Mode Redundant. The logic layout work and top-level chip assembly were done at IMEC (Leuven, Belgium), the contractor for rad-hard DARE cell layouts.

All flipflops in the logic are Heavy Ion Tolerant (HIT) cells. The clock and reset nets use Single Event Transient-tolerant cells exclusively, with drive-strength hardening. The final layout measures 18.5 x 14.5 mm, and contains 400 kgates of logic and 40 RAM instances. The large RAMs have Built-In Self-Test (BIST), as well as EDAC with single-bit error correction per 32 bit word [5].

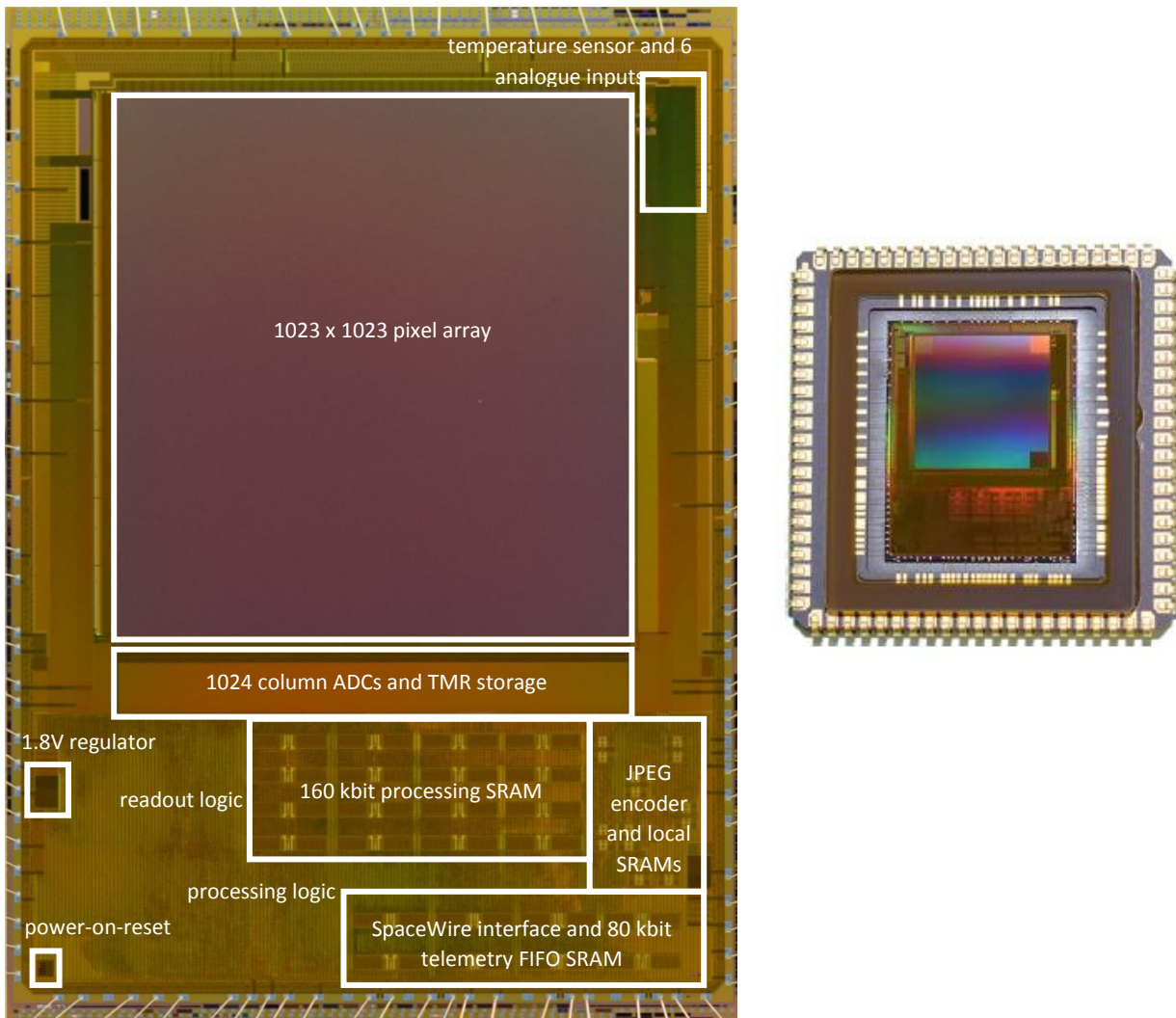


Figure 4: Micrograph of the Faintstar die with the indication of the functional building blocks as described in Figure 1 (Left). On the right is the packaged sensor.

The Faintstar device is packaged in a J-Leaded Ceramic Carrier (JLCC) well known from legacy star tracker sensors for space. A semi-custom (cavity only is custom) 84-pin package was designed, with embedded metal routing to connect the 100 FaintStar pads to the 84 package pins. The epoxy-glued glass is rad-hard Schott BK7G18, with anti-reflective coating on both sides. The cavity is N2-filled at 1 atmosphere (Figure 4). Two variants of FaintStar will be offered: one with LVDS SpaceWire and the other with 3.3 V CMOS level SpaceWire. The distinction will be made at assembly time, with wire-bond options.

5. MEASUREMENT RESULTS

Over 100 devices were measured over the last 2 years. The tests include the determination of the electro-optical parameters as well as the execution of a full space qualification campaign. The key electro-optical parameters are summarized in Table 1.

Table 1: Summary of the main parameters measured during functional evaluation.

Parameter	Units	Requirement	Typical Result
format			
array (pixels x pixels)	--	1024 x 1024	1023 x 1023
pixel size	µm	10	10
frame rate			
full frame rate, on-chip processing	frames/s	7	< 11.8
full frame rate, raw image output	frames/s	3.1	< 4.6
windowed frame rate	frames/s	> 20	> 20 ⁽¹⁾
electro-optical			
charge conversion gain	LSB/e-		0.032
full well charge	ke-	80	108
readout noise	e-	< 40	21
fixed pattern noise	e-	< 15	8
photo response non-uniformity	%	< 1.5	0.55
dark current, BOL	e-/s at 21°C	< 100	25
dark current non-uniformity, BOL	e-/s at 21°C		35
Average QE*FF over 400-700 nm	%	> 35	54
electrical			
ADC resolution	bit	11 and 12	11 and 12
power	mW	< 200	244 .. 325
ESD	kV (HBM)	> 1	2
external reference voltages		none	none
on-chip supply regulators		yes	yes

⁽¹⁾Frame rate depends on the actual number of windows and their relative positions.

The Quantum Efficiency (QE*FF) is given in Figure 5. Although the peak responsivity is somewhat lower than the other variants, this pixel is selected because the additional pixel design features are resulting in a lower dark current increase and a lower dark signal non-uniformity under the influence of ionizing radiation.

The following figures (Figure 6 a to f) demonstrate the imaging and processing capabilities of Faintstar. All images are real-life captures of the sensor. Figure 6-a shows the optical scene, which was generated through a diffuser and a paper mask with holes to create an impression of straylight. On top of this background, the internal bad pixel table was used to generate a synthetic image with ten stars and one extended object. The specific sensor, used in this experiment, has also one defective column and one defective row. The next images show how the centroids of the stars were obtained,

and how the measurement of the large object was executed, using all embedded functions present in the star tracker.

In Figure 6-b, we selected the 1-D moving average background filter, removing a large part of the bright background. This results in a near-black image with the stars, large object, and defective column preserved.

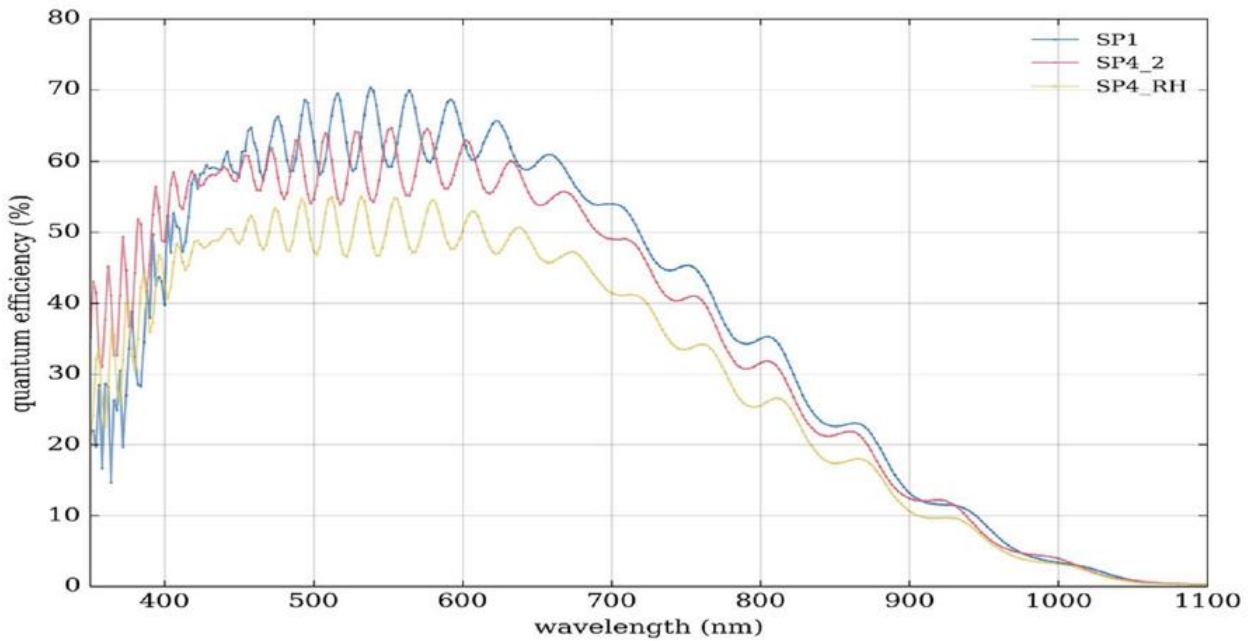


Figure 5: Quantum Efficiency times Fill Factor as a function of wavelength. The curve SP4_RH is representative for the present Faintstar version.

In Figure 6-c, the single-illuminated pixel filter removes the defective column, and further thresholding reduces the image to totally black with only the bright objects of interest remaining.

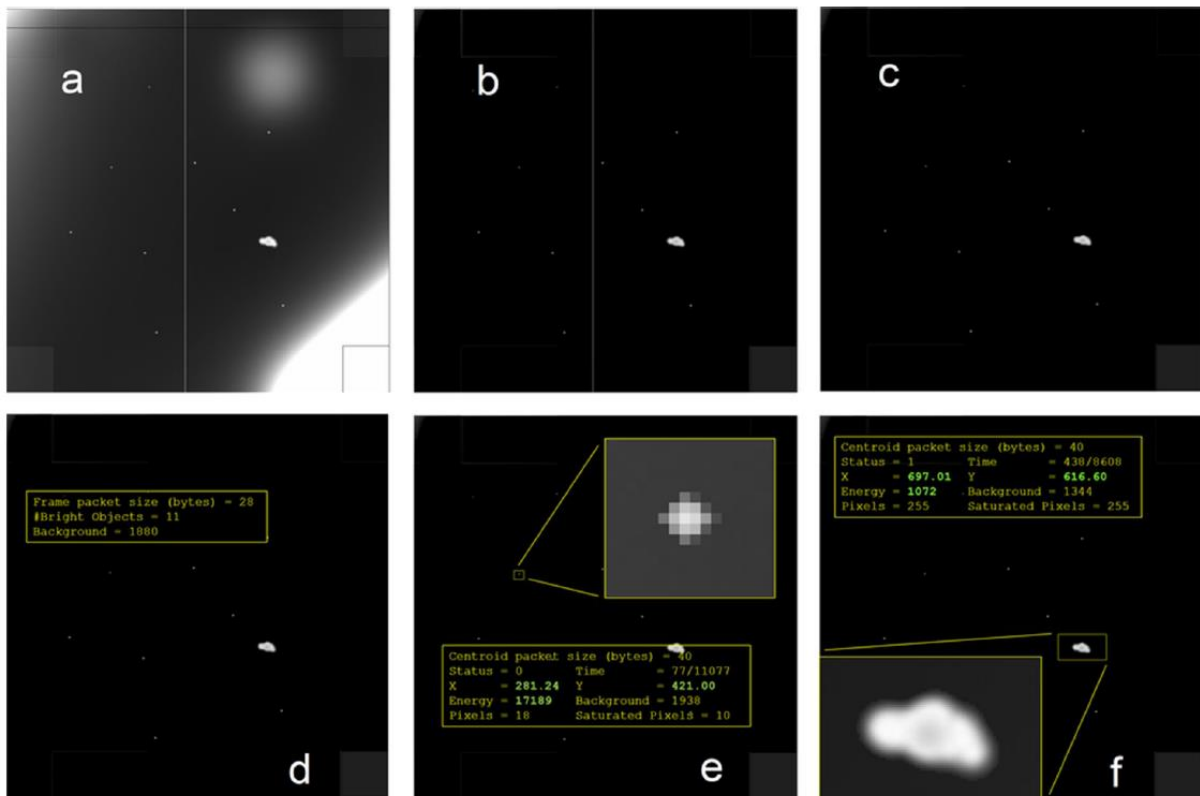


Figure 6: Demonstration of the Star image processing capability in the presence of stray light, 10 stars and 1 extended object.

The Pixels are also extensively tested for space radiation effects. The first test executed was the irradiation till 100 krad at the ^{60}Co facility of CEA in Saclay. The devices were tested powered, but unlocked. Almost all parameters of the device remained unchanged. The temporal noise, black level and Fixed Pattern Noise (FPN) are slightly increased, while – as could be expected – the major influence is seen on the Dark Current and the Dark Current Non-Uniformity (see Figure 7). After 168 hours at Room temperature half the effect is already disappeared and after 168h hours at 100 °C, most of the effects are annealed.

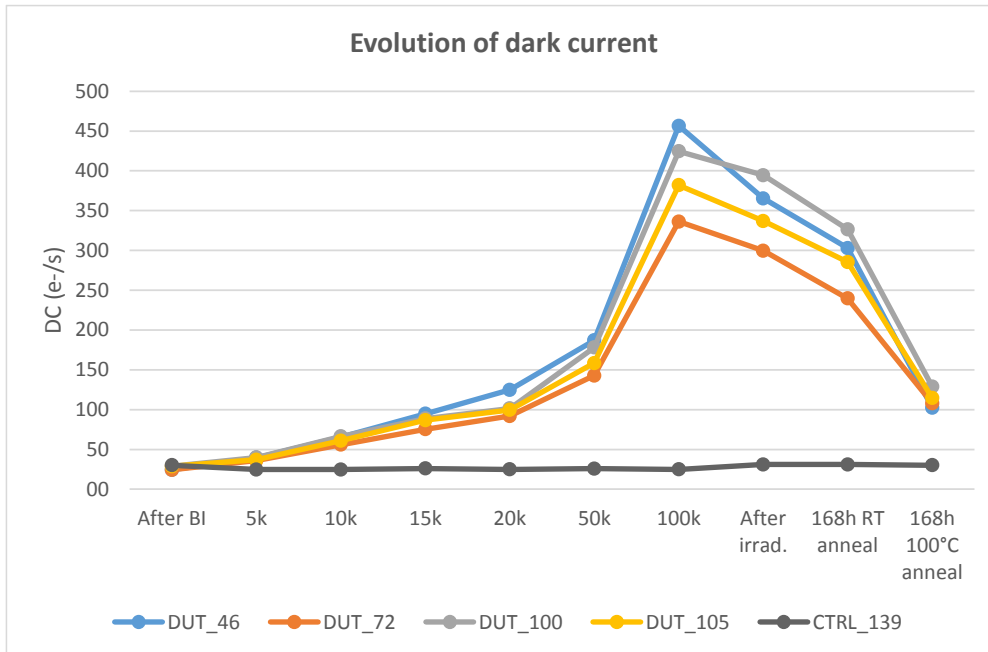


Figure 7: Dark current evolution as a function of TID Dose and annealing behavior.

The sensor was also irradiated with a 30 MeV proton beam at the LIF facility of Louvain-la-Neuve, Belgium. During the irradiation the devices was unpowered, and all pins were shortened. The sensor glass attenuated the energy of the protons to app. 23.5 MeV, this attenuation makes the results app. 10 % pessimistic, as the NIEL effect of 23.5 and 30 MeV protons is 10 % apart. Also, in this case the major effect of the radiation was observed on the dark current and the dark current non-uniformity parameters (see Figure 8).

SEE was also analyzed in the HIF facility of Louvain-la-Neuve, Belgium. No SEL was observed under the influence of 995 MeV Xe ions. Neither were SEU events observed in the flip-flop of the static registers and the core logic. The core logic itself is mildly sensitive to Single Event Transients in combinatorial cells, for LET values above 16 MeV/mg/cm². The internal RAM is only limited protected by word-level single and double error correction; consequently, SEU's were observed at all LET levels.

Samples of Faintstar have also undergone mechanical and environmental tests with good success. The tests include Sine, Random Vibration, and shock; temperature cycling and moisture resistance and hermeticity. Finally, the assembly quality and the solderability of the packaged device was tested as well.

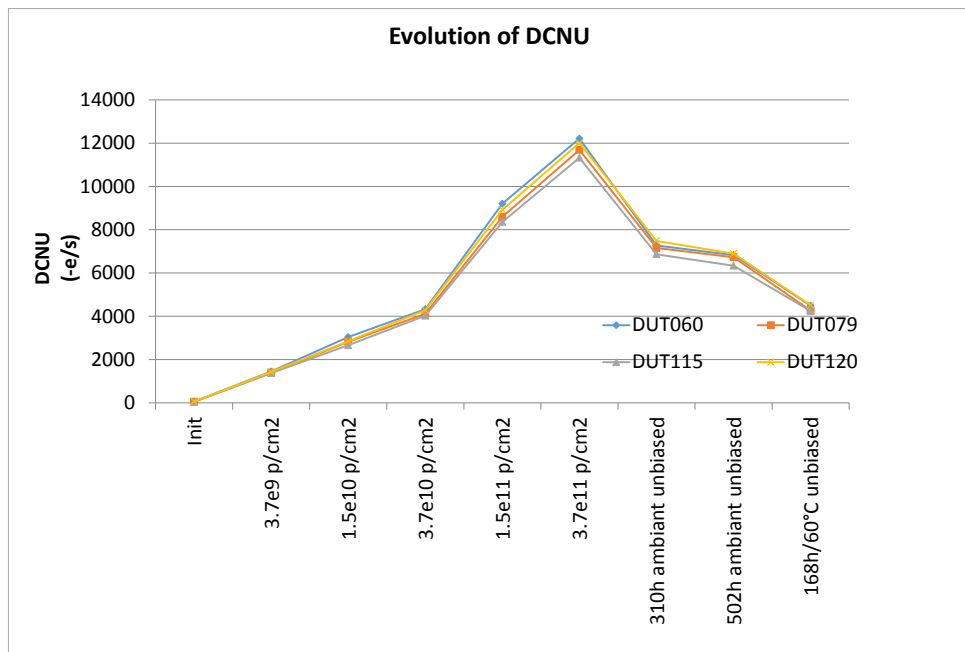


Figure 8: Dark current increase under 30 MeV proton irradiation, followed by Room Temperature and 60 °C anneal periods.

6. CONCLUSIONS

The Faintstar sensor is designed as a System-on-a-chip core star tracker device. It can be used as regular high-performance star-tracker with low component count as biasing and resistors are internal. more powerful is the use as star tracker with pre-processing function; the device removes the burden of the high data rate, low-level computations from the star tracker unit processor, reducing considerably the complexity of the star tracker subsystem. The chip has several versatile operating modes allowing raw and processed video, windowed operation, and full star centroiding operation.

The device shows good electro-optical performance with peak QE > 50 % and with low dark current; the power dissipation is also as expected. The device is packaged in a JLCC-84 package closed hermetically with a window. The device is fully qualified for mechanical and environmental excitations and has proven to withstand the space radiation environment.

The authors want to thank the involved staff at Cmosis/ams, Adveotec and ESA/ESTEC for their contribution and many helpful discussions.

7. REFERENCES

- [1] ESA contract 17235/03/NL/FM, Active Pixels for Star Trackers
- [2] W.Ogiers, K.Ruythooren, K.Van Wichelen, M.Dendoncker, S.Kowaltschek, B.Razgus, Faint Star – A Single-Chip STR Head – Prototype Results, GNC2017, 10th International ESA Conference on Guidance, Navigation, & Control Systems
- [3] W.Ogiers, S.Airey, Integrating additional functionality with APS sensors, 30th Annual AAS Guidance and Control Conference, Breckenridge, Colorado, 3-7 February 2007
- [4] P.Fidanzati, F.Boldrini, E.Moncini, W.Ogiers, A.Pritchard, S.Airey, S.Kowaltschek, Miniature Sun Sensor on a Chip Performance Evaluation, GNC2011, 8th International ESA Conference on Guidance, Navigation & Control Systems
- [5] S.Redant, R.Marec, L.Baguena, E.Liegeon, J.Soucarre, B.Van Thielen, G.Beeckman, P.Ribeiro, A.Fernandez-Leon, B.Glass Radiation Test Results on First Silicon in the Design Against Radiation Effects (DARE) Library, IEEE Trans. on Nuclear Science, 2005, vol. 52, no. 5